All-electron relativistic computations on the low-lying electronic states, bond length, and vibrational frequency of CeF diatomic molecule with spin-orbit coupling effects

Yusuke Kondo,[a] *Masato Kobayashi*,[b] *Tomoko Akama*,[b] *Takeshi Noro*,[b] and *Tetsuya Taketsugu**[b]

---

[a] *Yusuke Kondo*

Graduate School of Chemical Sciences and Engineering, Hokkaido University, Sapporo 060-0810, Japan

[b] *Masato Kobayashi, Tomoko Akama*, *Takeshi Noro, Tetsuya Taketsugu*

Department of Chemistry, Faculty of Science, Hokkaido University, Sapporo 060-0810, Japan

Corresponding author (Tetsuya Taketsugu)

E-mail: take@sci.hokudai.ac.jp

Abstract:

Ab initio all-electron computations have been carried out for Ce^+ and CeF, including the electron correlation, scalar relativistic, and spin-orbit coupling effects in a quantitative manner. First, the *n*-electron valence state 2nd-order multireference perturbation theory (NEVPT2) and spin-orbit configuration interaction (SOCI) based on the state-averaged restricted active space multiconfigurational self-consistent field (SA-RASSCF) and state-averaged complete active space multiconfigurational self-consistent field (SA-CASSCF) wavefunctions have been applied to evaluations of the low-lying energy levels of Ce^+ with $[Xe]4f^15d^16s^1$ and $[Xe]4f^15d^2$ configurations, to test the accuracy of several all-electron relativistic basis sets. It is shown that the mixing of quartet and doublet states is essential to reproduce the excitation energies. Then, SA-RASSCF(CASSCF)/NEVPT2+SOCI computations with the Sapporo(-DKH3)-2012-QZP basis set were carried out to determine the energy levels of the low-lying electronic states of CeF. The calculated excitation energies, bond length, and vibrational frequency are shown to be in good agreement with the available experimental data.

Introduction

A state-of-the art *ab initio* wavefunction theory has advanced for 60 years so as to treat various types of electronic structure systems quantitatively, and the target is now extended to the lanthanide (Ln) molecular system.[1] The magnetic properties of lanthanide single–molecule magnets attract a lot of attentions due to the possibility of a useful application such as magnetic resonance contrast agents.[2] Soncini and coworkers[3] have very recently proposed an *ab initio* sophisticated approach to the calculations of the electronic structures and magnetic properties of lanthanide complexes, considering both the spin-orbit coupling and ligand-field effects. The lanthanide containing molecules and complexes have a common characteristic of partially-filled atomic orbital (AO)-like 4f orbitals, which often requires some state-average treatments in orbital determining step, and balanced treatments for the static and dynamic correlation effects as well as the scalar and spin-orbit relativistic effects. For the lanthanide compounds, the relativistic effective core potential (RECP) approach[4] has been widely used for a long time. Yabushita and coworkers[5] employed three different RECPs to investigate the low energy spin-orbit multiplet terms of trivalent lanthanide cations, Ln^{3+}, including the spin-orbit coupling effect explicitly by the full-variational spin-orbit configuration interaction (SOCI) method, and found that semi-core correlations in the 4d, 5s, and 5p shells are significant to reproduce the higher LS terms. One of the authors (TT) employed a state-averaged complete active space multiconfigurational self-consistent field (SA-CASSCF) method with the RECP to discuss the electronic and geometric structures of a series of the lanthanide trihalides, LnX_3 (Ln = La-Lu; X = F, Cl), including spin-orbit coupling effect explicitly.[6]

The electronic structures of a series of low valency lanthanide monofluorides, LnF, have been known for a long time in the experimental community through the earlier work by the Gotkis group[7] and by the Field group.[8-10] The bonding nature of LnF is ionic where F^- is bound to Ln^+. The early lanthanide atom, Ce, has the ground-state configuration of $[Xe]4f^15d^16s^2$, while the Ce^+ ion has the ground-state configuration of $[Xe]4f^15d^2$.[11] Interestingly, Ce^+ in the ground state of CeF has an electron configuration of $[Xe]4f^15d^16s^1$, which corresponds to the excited-state configuration of Ce^+.[8,9] For CeF, two low-lying excited states were observed with excitation energies of 0.087 eV (Ω = 4.5) and 0.186 eV (Ω = 3.5) by selectively detected fluorescence excitation and dispersed fluorescence spectroscopy,[10] where Ω denotes a quantum number for the total electronic angular momentum around the molecular axis. To study the low-lying excited states and spectroscopic constants of CeF, Tatewaki and coworkers[12,13] employed a four-component relativistic method with the single and double excitation configuration interaction (SDCI) and multi-configurational quasi-degenerate perturbation theory (MCQDPT), based on the reduced frozen-core approximation. In their calculations, good agreement with the experimental data was obtained for the Ce-F equilibrium bond length and stretching frequency, while the excitation energies were calculated to be 0.104 and 0.312 eV for the Ω = 4.5 and Ω = 3.5 states, respectively, which are slightly larger than the corresponding experimental values (0.087 eV (Ω = 4.5) and 0.186 eV (Ω = 3.5)).

Recently, the sophisticated two-component relativistic methods such as the relativistic scheme by eliminating small components (RESC)[14] and Douglas-Kroll-Hess (DKH) methods[15,16] have been proposed. Along this two-component relativistic approach, several all-electron relativistic basis sets have been developed for lanthanides, such as Sapporo-DKH3-*X*ZP-

2012,[17] ANO-RCC,[18] and cc-pwCV*X*Z[19] (*X* = D, T, and Q). Noro and Sekiya have developed a family of Sapporo basis sets for the elements in a periodic table systematically.[17,20-22] The Sapporo basis sets are designed in a correlation-consistent manner based on a segmented-contraction scheme, and thus, the size is compact and good accuracy is expected. Very recently, Schoendorff and Wilson[23] employed the all-electron Sapporo-DKH3-TZP-2012 and Sapporo-TZP-2012 basis sets in the CASSCF and coupled-cluster calculations with an infinite order two-component method for the scalar relativistic effect to investigate the spectroscopic constants of the ground and low-lying excited states of lanthanide monofluorides, NdF and LuF. In their calculations, the significance of core correlation was verified to reproduce the bond dissociation energies. However, all-electron computations for the lanthanide compounds are still limited.

In this paper, we report all-electron *ab initio* multiconfigurational/mutireference study on the ground and low-lying excited states of CeF, based on a two-component relativistic scheme. We first examine the ground and low-lying excited states of Ce^+ systematically, and then, discuss the excited states and spectroscopic constants of CeF.

Computational details

First, we calculated the excitation energies of the nearly-degenerate low-lying quartet states of Ce^+ that originate from the ground-state configuration, $[Xe]4f^15d^2$, and from the excited-state configuration, $[Xe]4f^15d^16s^1$, with RECP and all-electron computations. In the RECP calculations, Dolg's RECP[24] combined with def2-QZVPP (11s8p6d5f) basis set[25] was employed, while in the all-electron computations, ANO-RCC (12s11p8d7f4g2h),[18] Sapporo-DKH3-QZP-2012 (13s11p9d7f4g3h1i),[17] and cc-pwCVQZ (13s12p10d9f7g4h1i)[19] relativistic basis sets were employed with the third-order Douglas-Kroll one-electron integrals[26] for the scalar relativistic effects. The numbers of basis functions are 100, 192, 222, and 282 for def2-QZVPP, ANO-RCC, Sapporo-DKH3-QZP-2012, and cc-pwCVQZ, respectively; def2-QZVPP and ANO-RCC were designed so that the correlated orbitals are 4f, 5spd (5s, 5p, 5d), and 6s whereas Sapporo-DKH3-QZP-2012 and cc-pwCVQZ were designed so that the correlated orbitals are 4spdf (4s, 4p, 4d, 4f), 5spd, and 6s. All the electronic structure calculations were carried out with the Molpro2012 program package.[27,28]

For Ce^+, the state-averaged restricted active space self-consistent field (SA-RASSCF) method[29] was employed for 70 quartet states of the $[Xe]4f^15d^2$ configuration and 35 quartet states of the $[Xe]4f^15d^16s^1$ configuration separately, with the active space of 3 electrons in 13 orbitals. The state-average scheme is used to get a set of orbitals for describing the nearly-degenerate multi-states equally, and thus, the obtained orbitals are not optimal for the respective states. It is noted that the state-average scheme can reproduce the degeneracy of the electronic states correctly. Succeedingly, the *n*-electron valence state 2nd-order multireference perturbation theory

(NEVPT2) with a strongly-contracted scheme[30-32] was employed based on the SA-RASSCF zeroth-order wavefunction to estimate the dynamic correlation energy for the respective SA-RASSCF states. In the NEVPT2 calculations, 4f, 5spd, and 6s orbitals were included to estimate the dynamic correlation energy for def2-QZVPP and ANO-RCC basis sets, while 4spdf, 5spd, and 6s orbitals were included as correlated orbitals for Sapporo-DKH3-QZP-2012 and cc-pwCVQZ basis sets. The additional calculation with Sapporo-DKH3-QZP-2012 involving only 4f, 5spd, and 6s as correlated orbitals was also performed to show the core-correlation effects explicitly. In the Breit–Pauli Hamiltonian scheme,[33] the spin-orbit coupling matrix was generated for 280 electronic states (from the ground-state configuration with quartet) and for 140 electronic states (from the excited-state configuration with quartet) based on the SA-RASSCF wavefunction. Then, the SA-RASSCF energies for the respective electronic states in the diagonal terms were replaced with the corresponding NEVPT2 energies, followed by a diagonalization of the resultant spin-orbit coupling matrix to evaluate the energy levels of the spin-orbit-coupled states (referred to as spin-orbit configuration interaction: SOCI). The similar approach was applied to *ab initio* calculations of the low-lying states of PtCN/PtNC and PdCN/PdNC.[34] The present SA-RASSCF/NEVPT2+SOCI computations were also performed for 420 states including both $[Xe]4f^{1}5d^{2}$ and $[Xe]4f^{1}5d^{1}6s^{1}$ configurations of quartet to discuss the mixing of these two ensembles of different electronic configurations.

The experimental data[11] indicate that the ground state of Ce^{+} is quartet ($^{4}H_{7/2}$) with a considerable mixing of the doublet lowest state ($^{2}G_{7/2}$). To examine a mixing with the doublet states, we carried out additional calculations for selected low-lying quartet and doublet states by applying the SA-CASSCF/NEVPT2+SOCI approach. It is noted that SOCI calculations including

doublet and quartet states using the MOLPRO program[27,28] require the SA-CASSCF wavefunction (SA-RASSCF does not work). The SA-CASSCF active space in this calculation is defined as 3 electrons in 12 orbitals (seven 4f and five 5d orbitals).

Next, all-electron *ab initio* calculations were carried out for the ground and low-lying excited states of CeF with the Sapporo basis sets (Sapporo-DKH3-QZP-2012 for Ce and Sapporo-QZP-2012[20] for F). The energy levels of the excited states of CeF which originate from 280 quartet states ($[Xe]4f^{1}5d^{2}$) and 140 quartet states ($[Xe]4f^{1}5d^{1}6s^{1}$) were calculated at the equilibrium structure by the SA-RASSCF/NEVPT2+SOCI approach. The SA-RASSCF active space consists of 13 orbitals (4f, 5d, 6s) of the Ce atom, while 4spdf, 5spd, and 6s orbitals of Ce and 2sp orbitals of F were included as correlated orbitals in the NEVPT2 calculations. The additional calculations including doublet states were also performed by the SA-CASSCF/NEVPT2+SOCI approach. The Ce-F bond length and stretching frequency were evaluated by solving the one-dimensional ro-vibrational Schrödinger equation, using the VIBROT code in MOLCAS.[35]

Results and discussion

A. Excited-state calculations of the low-lying electronic states of Ce^+

We first discuss the electron correlation effects on the relative energies of the low-lying quartet states of Ce^+. The atomic terms, ^{2S+1}L (L and S denote quantum numbers of the resultant orbital angular momentum and the resultant spin angular momentum, respectively), are ^{4}S, ^{4}P, ^{4}D×2, ^{4}F×2, ^{4}G×2, ^{4}H, and ^{4}I for the ground-state configuration [Xe]4f^{1}5d^2 and ^{4}P, ^{4}D, ^{4}F, ^{4}G, and ^{4}H for the excited-state configuration [Xe]4f^{1}5d^{1}6s^1. Due to the spin-orbit coupling effect, these electronic states mix in with each other, and the spin-orbit coupled states, $^{2S+1}L_J$, are classified according to the total angular momentum quantum number J ($|L - S| \leq J \leq L + S$). Here, in order to discuss the electron correlation effects on the relative energies of the low-lying electronic states, the excitation energies for the spin-orbit uncoupled states, $E(^{2S+1}L)$, are compared with each other. As the reference energies, the experimental excitation energies for the spin-orbit uncoupled states (J-averaged value) were estimated from the experimental energy levels of the spin-orbit coupled states, $E_{\mathrm{exp}}(^{2S+1}L_J)$, by the following equation:

$$E\left(^{2S+1}L\right) = \frac{\sum_{J=|L-S|}^{L+S}(2J+1)E_{\mathrm{exp}}\left(^{2S+1}L_J\right)}{(2S+1)(2L+1)} \qquad (1)$$

This is of course an approximation formula in the sense that it does not take account of the contributions from the other ^{2S+1}L states in $E_{\mathrm{exp}}(^{2S+1}L_J)$, and actually in the experimental data book,[11] a J-averaged value is missing for some electronic terms.

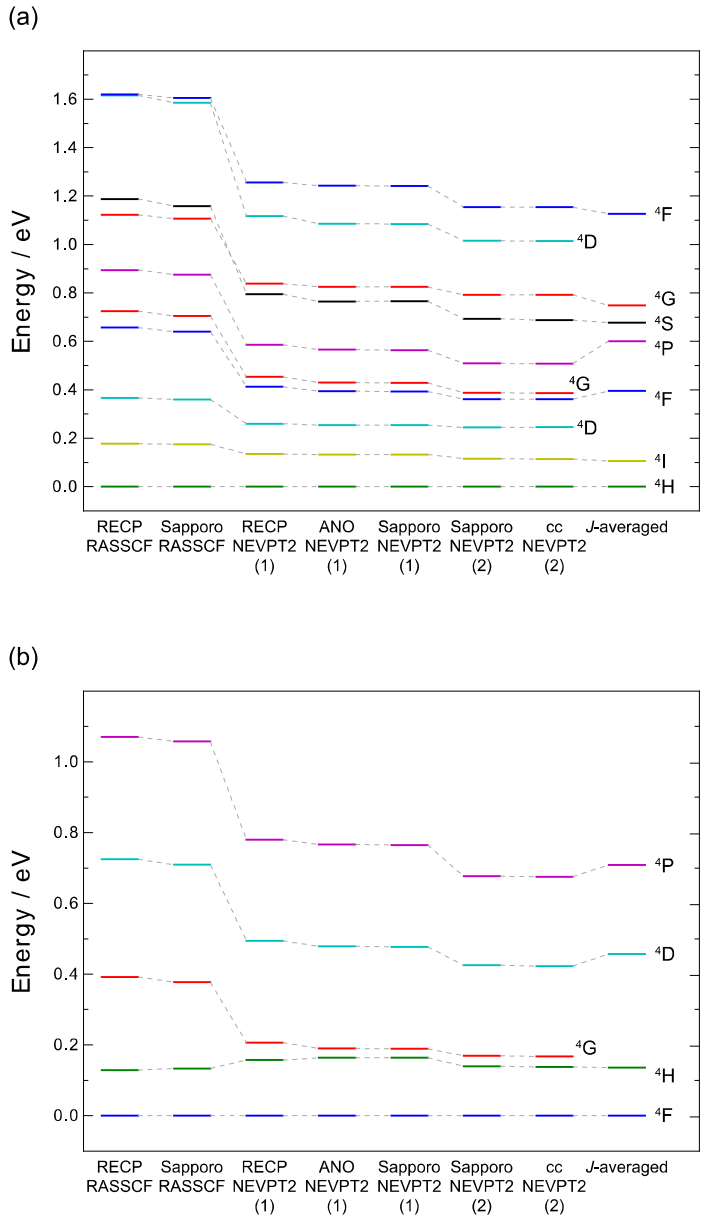

Figure 1. The calculated energy levels for the low-lying electronic states of Ce^{+} that originate from (a) the ground-state configuration, $[Xe]4f^{1}5d^{2}$, and (b) the excited-state configuration, $[Xe]4f^{1}5d^{1}6s^{1}$; the correlated orbitals in NEVPT2 calculations are (1) 4f, 5spd, and 6s and (2) 4spdf, 5spd, and 6s. The *J*-averaged values calculated from the available experimental data[11] are also shown.

Figure 1 shows the energy levels for (a) the electronic states of Ce^+, generated from the ground-state configuration, $[Xe]4f^15d^2$, and (b) those from the excited-state configuration, $[Xe]4f^15d^16s^1$, relative to the lowest electronic state of the respective configurations, calculated by the SA-RASSCF/NEVPT2 method with several basis sets. The *J*-averaged values calculated from available experimental data[11] are also given. As is shown in Fig. 1, the energies of 70 states from the ground-state configuration are ranged within 1.2 eV, while those of 35 states from the excited-state configuration are ranged within 0.7 eV, indicating that a lot of electronic states are lying within a small energy range. As the results of the calculations, it is verified that the calculated energy levels have an appropriate degenerate feature in all computations, and thus, the respective atomic terms are indicated by a single line in Fig. 1.

In Fig. 1, the SA-RASSCF can almost reproduce the order of the electronic states for both ground-state and excited-state configurations from the experiment (only ^4S and ^4G states from the ground-state configuration are inconsistent with the experiment), although the excitation energies are overestimated in most cases. The NEVPT2 improves the SA-RASSCF energetics drastically, and the calculated excitation energies are in good agreement with the corresponding experimental values. In the NEVPT2 calculations, two different correlated orbital sets were employed, i.e., (1) 4f, 5spd, and 6s (RECP/def2-QZVPP, ANO-RCC, and Sapporo-DKH3-QZP-2012) and (2) 4spdf, 5spd, and 6s (Sapporo-DKH3-QZP-2012 and cc-pwCVQZ), and the comparison of these two different calculations shows that, at least, the electron correlation from 4f, 5spd, and 6s electrons needs to be included for quantitative discussions of the energetics, and that the dynamic correlation effects due to the inner-shell 4spd electrons reduce the excitation energies slightly, resulting in better agreement with the experimental values. The energy levels of the ^4F and ^4S

states from the ground-state configuration are much improved by the inner-shell electron correlation effect, while the ^{4}P state from the ground-state configuration shows a slightly large difference between the NEVPT2 value and experimental value. This difference may be ascribed to the *J*-averaged scheme from the experimental raw data, which do not consider the contributions from the other spin states.

The all-electron and RECP calculations show very similar energetics for the excitation energies, and thus, it is concluded that the all-electron and RECP basis sets employed in this study have a superior performance at the respective computational levels. The NEVPT2 calculations with the Sapporo-DKH3-QZP-2012 and cc-pwCVQZ basis sets (including 4spdf, 5spd, and 6s as correlated orbitals) show a similar accuracy in the energetics. The number of basis functions in the Sapporo-DKH3-QZP-2012 and cc-pwCVQZ basis sets are 222 and 282, respectively, and thus Sapporo-DKH3-QZP-2012 is a more compact and more efficient basis set. **Table 1** shows the CPU times for each step of molecular integral, spin-restricted Hartree-Fock (RHF), SA-RASSCF, and NEVPT2 (for one state) computations, using four different basis sets. The computational time for SA-RASSCF increases as the number of basis function grows, but as to the computations for the molecular integral, Sapporo-DKH3-QZP-2012 shows a shorter CPU time than ANO-RCC. This is because Sapporo-DKH3-QZP-2012 was developed by a segmented contraction scheme, while the other basis sets were developed by a general contraction scheme. On the other hand, the NEVPT2 calculation with a strongly-contracted scheme shows almost the same CPU time for any all-electron basis sets, since the correlation energy is estimated on the basis of the density matrix from the SA-RASSCF calculation.[32] In the following discussions, we employed the Sapporo-DKH3-QZP-2012 basis set that is compact and provides an equivalently accurate result to the cc-

pwCVQZ basis set.

Table 1. The CPU times (in second) for molecular integral, RHF, SA-RASSCF, and one-state NEVPT2 computations, measured on a single-node computer equipped with one Intel Xeon W3690 (3.46 GHz) processor using one CPU core, using four different basis sets. The number in parenthesis after the basis set denotes the number of basis functions.

	integral	RHF	SA-RASSCF	NEVPT2
RECP (100)	6.2	0.3	3.5	355.4
ANO-RCC (192)	24.6	1.5	13.4	355.7
Sapporo-QZP (222)	22.9	2.1	19.1	358.8
cc-pwCVQZ (282)	147.0	5.6	37.8	382.6

Here, the relative energies for the electronic states derived from the ground-state configuration and those from the excited-state configuration were discussed. **Figure 2** shows the calculated and experimental *J*-averaged energy levels of the related electronic states where the zero energy is set to the ground state. The energy difference of the lowest state with the $[Xe]4f^{1}5d^{2}$ configuration (^{4}H) and the lowest state with the $[Xe]4f^{1}5d^{1}6s^{1}$ configuration (^{4}F) was reported to be 0.209 eV in the experiment.[11] This small energy difference suggests that the electronic states from the ground-state and excited-state configurations mix in with each other, and such a mixing can occur over the electronic states with the same symmetry representations. In the SA-RASSCF/NEVPT2 calculations for both $[Xe]4f^{1}5d^{2}$ and $[Xe]4f^{1}5d^{1}6s^{1}$ configurations, the SA-RASSCF orbitals were optimized with equally averaging ensembles originating from both

configurations. The energy difference of the ^{4}H ([Xe]4f^{1}5d^2) and ^{4}F ([Xe]4f^{1}5d^{1}6s^1) states was calculated to be 0.292 eV, showing a slightly larger value than the experimental *J*-averaged value, 0.209 eV. To examine the mixing of the electronic states between these two configurations, we also investigated the CI coefficients of the SA-RASSCF wavefunction. Even in the most largely mixing case, the lowest and the second lowest ^{4}F states mix in with 2.0%, and the lowest and the second lowest ^{4}G states mix in with 0.025%, and thus, the mixing of these two configurations is not strong.

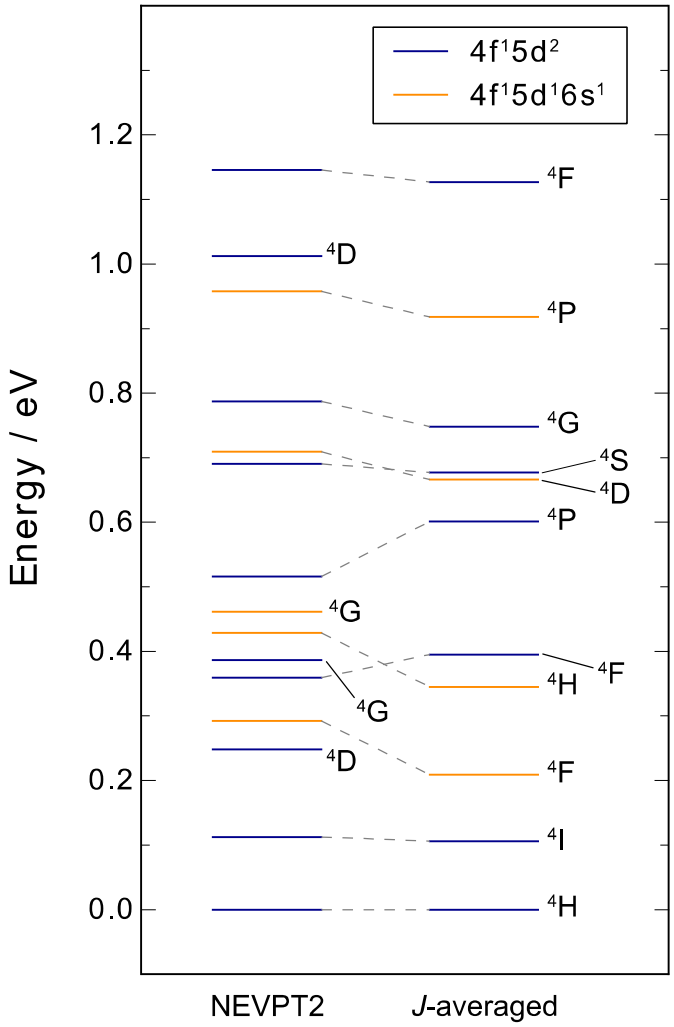

Figure 2. The comparison of the low-lying energy levels of Ce^{+} between the calculated (at SA-RASSCF/NEVPT2 with Sapporo-DKH3-QZP-2012) and *J*-averaged values calculated from the experimental data.[11] The electronic states shown here are only the quartet states derived from the ground-state configuration ([Xe]$4f^{1}5d^{2}$; in blue) and from the excited-state configuration ([Xe]$4f^{1}5d^{1}6s^{1}$; in orange).

Next, the energy levels of the spin-orbit coupled states of Ce^+ were calculated by the SOCI method. When considering only the quartet states, the number of independent states of the ground-state configuration ($[Xe]4f^15d^2$) amounts to 280 (= 70 × 4), while the number of independent electronic states of the excited-state configuration ($[Xe]4f^15d^16s^1$) amounts to 140 (= 35 × 4). **Figure 3** shows the energy levels of (a) the spin-orbit coupled states calculated from the ground-state configuration of quartet and (b) those from the excited-state configuration of quartet at the SA-RASSCF and SA-RASSCF/NEVPT2 levels, as well as the available experimental energy levels.[11] As discussed above, the SA-RASSCF method has a tendency to overestimate the excitation energies, while the NEVPT2 method reduces the excitation energies as a whole, approaching to the experimental values in the respective ensembles. The electronic states from the ground-state configuration lie within a range of 1.6 eV, while those from the excited-state configuration lie within a range of 1.0 eV.

(a)

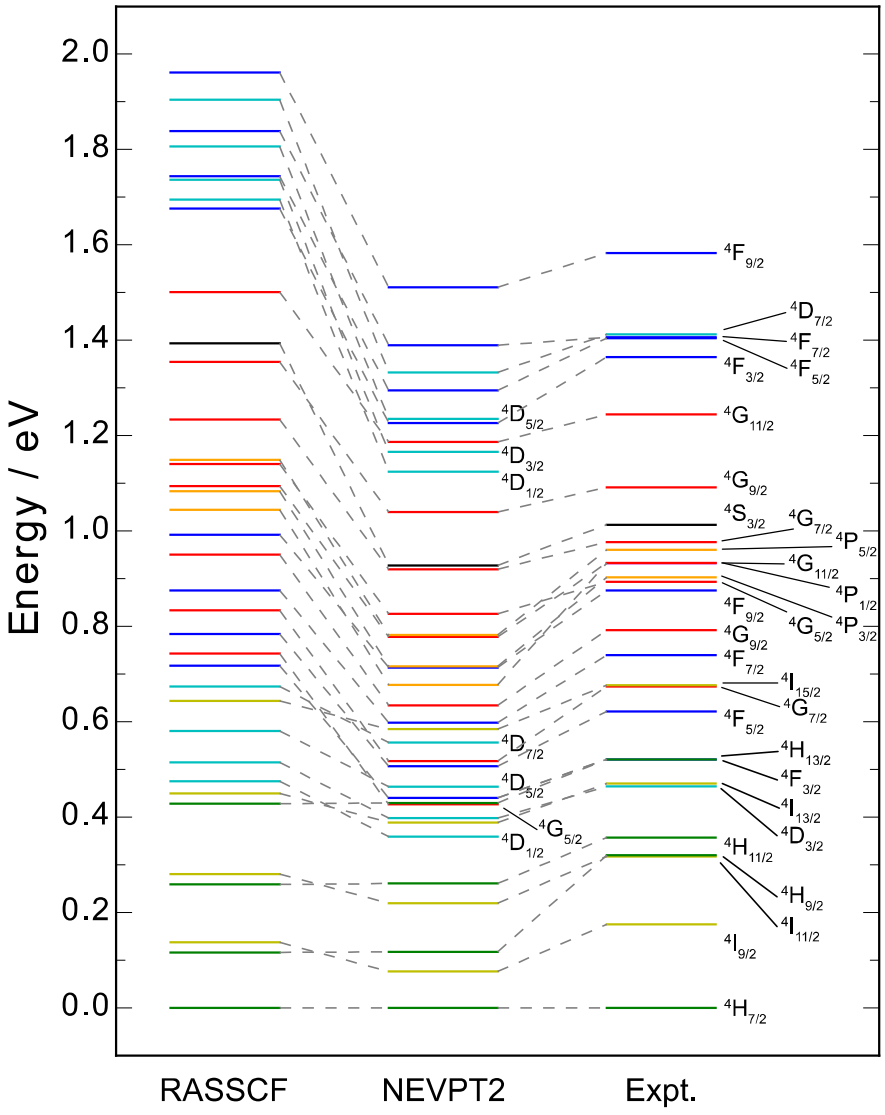
Energy / eV
2.0
1.8
1.6
1.4
1.2
1.0
0.8
0.6
0.4
0.2
0.0
RASSCF
NEVPT2
Expt.
4F9/2
4D7/2
4F7/2
4F3/2
4F5/2
4G11/2
4D5/2
4D3/2
4D1/2
4G9/2
4S3/2
4G7/2
4P5/2
4G11/2
4P1/2
4F9/2
4G5/2
4P3/2
4G9/2
4F7/2
4I15/2
4G7/2
4F5/2
4H13/2
4D7/2
4F3/2
4D5/2
4I13/2
4G5/2
4D3/2
4D1/2
4H11/2
4H9/2
4I11/2
4I9/2
4H7/2

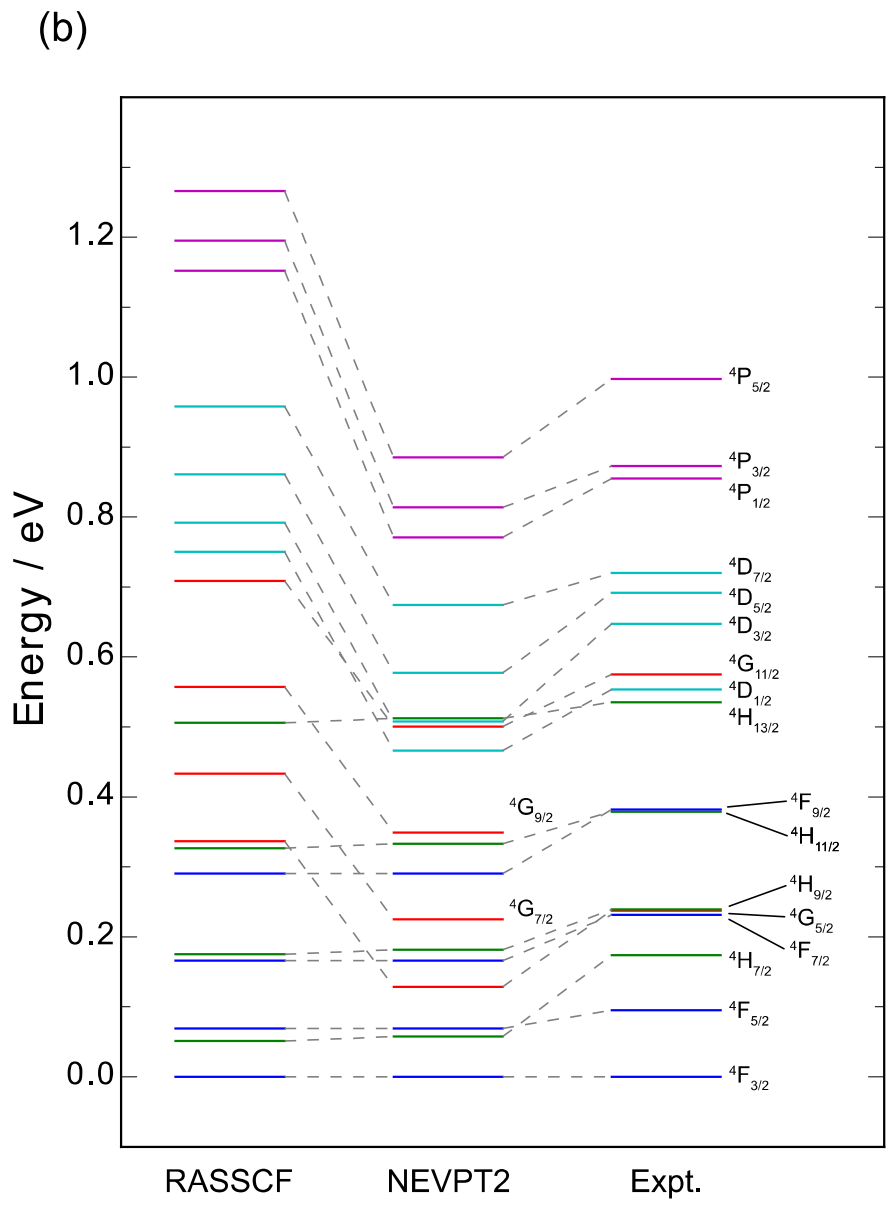

Figure 3. The SA-RASSCF, SA-RASSCF/NEVPT2, and experimental[11] energy levels of the ground and low-lying excited states of Ce^{+} which explicitly consider the spin-orbit coupling effects: (a) the electronic states from the ground-state configuration ($[Xe]4f^{1}5d^{2}$) and (b) the electronic states from the excited-state configuration ($[Xe]4f^{1}5d^{1}6s^{1}$).

In Fig. 3, qualitative agreement was obtained between the calculated and experimental energy levels, but in some cases the order in energy levels are different between the calculation and experiment. For example, in Fig. 3a, the energy level of the ^{4}P state is split to $^4P_{1/2}$, $^4P_{3/2}$, and $^4P_{5/2}$ by the spin-orbit coupling effect, and the order of the energy levels shows $E_{\mathrm{NEVPT2}}(^4P_{1/2}) < E_{\mathrm{NEVPT2}}(^4P_{3/2}) < E_{\mathrm{NEVPT2}}(^4P_{5/2})$, while experimentally the order was reported as $E_{\mathrm{exp}}(^4P_{3/2}) < E_{\mathrm{exp}}(^4P_{1/2}) < E_{\mathrm{exp}}(^4P_{5/2})$.[11] This irregular order suggests the necessity to consider the contribution from the other spin states such as doublet, sextet, etc. It is noted that both the ground-state and excited-state configurations, [Xe]4f^{1}5d^2 and [Xe]4f^{1}5d^{1}6s^1, also generate an ensemble of doublet states with similar energies to the quartet states. To discuss the effect of a mixing from the doublet states, we need to employ not SA-RASSCF but SA-CASSCF method in SOCI calculations due to a requirement of the MOLPRO program.[27,28] The employment of the SA-CASSCF method implies an appearance of many electronic states of different types of electronic configurations in the state-averaged solutions, and thus, we carried out SA-CASSCF calculations only for the quartet and doublet states originating from the ground-state configuration, [Xe]4f^{1}5d^2, by eliminating 6s orbital from the active space (only 4f and 5d are included in the active space), and in addition to the 280 (= 70 × 4) quartet states, only a part of the low-lying doublet states (^{2}G, ^{2}F, and ^{2}S) were involved in the SA-CASSCF/NEVPT2+SOCI calculations. The results are shown in Fig. 4 where only the energy levels of the quartet-dominant electronic states are plotted. By including the doublet states, agreement between theory and experiment is drastically improved, especially in the lowest energy region. As for the order of $^4P_{1/2}$, $^4P_{3/2}$, and $^4P_{5/2}$ states mentioned above, the correct order is reproduced by including the spin-orbit coupling effects in Fig. 4. The present results suggest the significance of an involvement of all the electronic states of spin

multiplicities related to the target electronic configuration in the present SA-CASSCF/NEVPT2+SOCI approach. The same discussions will be given for CeF in the following section.

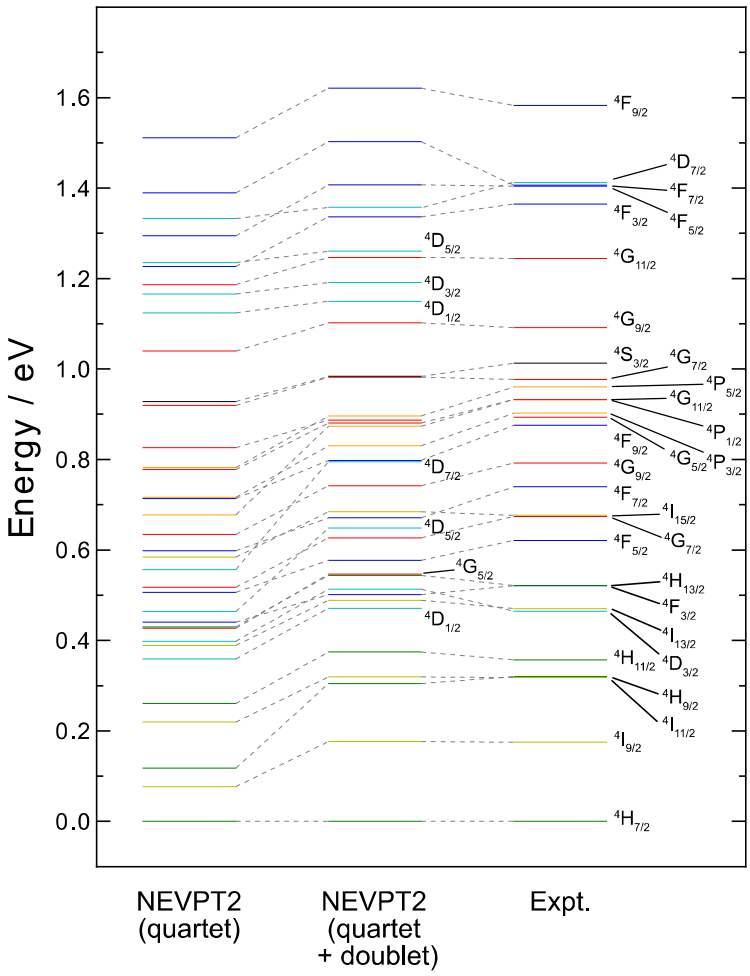

Figure 4. The NEVPT2 and experimental[11] energy levels of the ground and low-lying excited states of Ce^+ which originate from the ground-state configuration ($[Xe]4f^15d^2$). As for NEVPT2 results, two different calculated results are shown (SA-RASSCF/NEVPT2 for quartet and SA-CASSCF/NEVPT2 for quartet and doublet) where the energy levels in the left (NEVPT2 (quartet)) are the same as those of the middle one in Fig. 3a.

B. Excited states, bond length, and vibrational frequency of CeF

In the last section, it was verified that the SA-CASSCF/NEVPT2+SOCI approach with the Sapporo-DKH3-QZP-2012 basis sets can reproduce the energy levels of the low-lying electronic states of Ce^+ quantitatively, through a comparison with the experimental data. In this section, we first discuss the energy levels of the low-lying excited states of CeF calculated at SA-RASSCF/NEVPT2 with the Sapporo-DKH3-QZP-2012 basis set for Ce and the Sapporo-QZP-2012 basis set for F (referred to as Sapporo-QZP), followed by the SOCI calculation, to examine how the quasi-degenerate electronic states of Ce^+ change upon a formation of the CeF diatomic molecule. The bond length and vibrational frequency in the ground and excited states of CeF were also evaluated to discuss the accuracy of the present approach through a comparison with the available experimental data.[10,36]

In a CeF diatomic molecule, F^- has a complete closed-shell configuration like a noble gas atom, and thus, the electronic structures of the Ce part in CeF are approximately represented by those of Ce^+, perturbed by F^-. **Figure 5** shows the energy levels of those electronic states of $[Xe]4f^15d^16s^1$ and $[Xe]4f^15d^2$ configurations of Ce^+ (without SOCI) and CeF (without and with SOCI) where the energies are given relative to the lowest state of the respective species. In this calculation, the interatomic distance Ce-F was fixed at the experimental value, 2.048 Å,[36] and 35 states from the $[Xe]4f^15d^16s^1$ configuration (shown in blue) and 70 states from the $[Xe]4f^15d^2$ configuration (shown in orange) were solved in a state-average scheme. It is known that, in CeF, the energies of the electronic states of the $[Xe]4f^15d^2$ configuration are raised up and $[Xe]4f^15d^16s^1$ becomes the ground-state configuration, although $[Xe]4f^15d^2$ is the ground-state configuration in the isolated Ce^+.[8,9] This tendency was reproduced in our calculations.

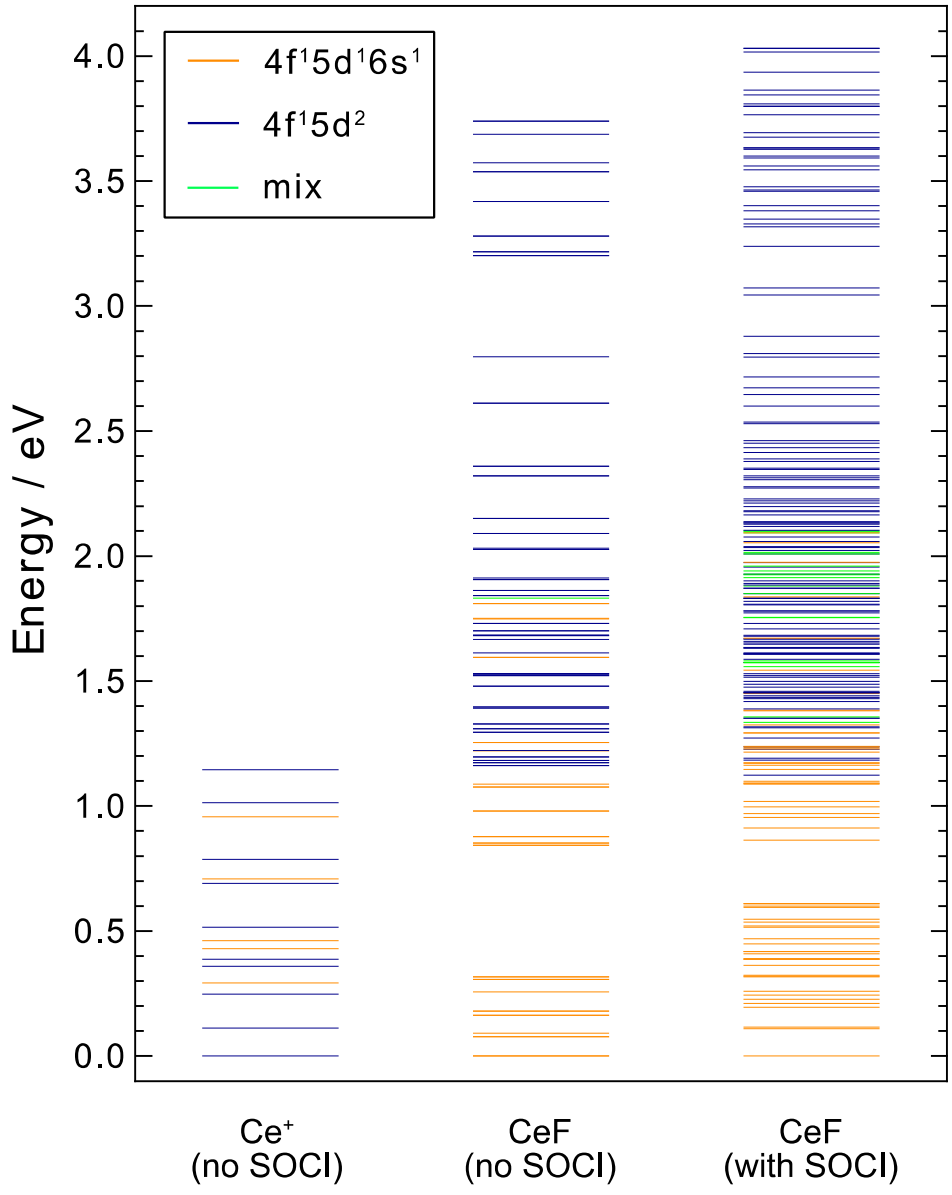

Figure 5. The energy levels of the low-lying electronic states of Ce^+ (without SOCI; the same as those in Fig. 2) and CeF (without and with SOCI), derived from the $[Xe]4f^15d^16s^1$ and $[Xe]4f^15d^2$ configurations of the Ce^+ part, calculated at the SA-RASSCF/NEVPT2 level with the Sapporo-QZP basis sets. The calculations for CeF were performed at the experimental bond length, r(Ce-F) = 2.048 Å.[36]

As shown in Fig. 5, 105 electronic states in Ce^+ are lying very crowdedly in a range of 0–1.2 eV, while in CeF without SOCI, the energy range of these states expands largely so that the electronic states of the $[Xe]4f^15d^16s^1$ configuration lie in a range of 0–1.8 eV while the electronic states of the $[Xe]4f^15d^2$ configuration lie in a range of 1.2–3.8 eV. The state mixing between these two configurations occurs very rarely, and only one state shows a mixing of more than 30%, indicated by green line. In Fig. 5, the electronic states from the $[Xe]4f^15d^16s^1$ configuration without SOCI (in orange) split to three groups with a range of 0–0.32 eV, 0.84–1.3 eV, and 1.6–1.8 eV. This grouping is related to the magnetic quantum number of the occupied 5d orbital in $[Xe]4f^15d^16s^1$ configuration: $5d_{\pm2}$ ($d_{x^2-y^2}$ or d_{xy}) in the lowest group, $5d_{\pm1}$ (d_{xz} or d_{yz}) in the second lowest group, and $5d_0$ (d_{z^2}) in the highest group. This order of 5d orbitals can be understood by considering the Coulomb repulsion between F^- and an electron in 5d orbitals; due to a spatial distribution of 5d orbitals, the order in a repulsion force from F^- should be $5d_0 > 5d_{\pm1} > 5d_{\pm2}$. It should be noted that 4f-electron is lying closer to the nucleus than 5d-electron. The order of energy in the electronic states derived from the $[Xe]4f^15d^2$ configuration can also be explained by considering a spatial distribution of singly-occupied 5d orbitals.

Hence, we discuss the reason why the ground-state configuration changes as $[Xe]4f^15d^2$ in Ce^+ to $[Xe]4f^15d^16s^1$ in CeF. The difference in these two configurations is occupation numbers in 5d and 6s orbitals. In previous theoretical studies[7,12,13] contour maps of densities of the valence spinors in the ground state were shown for understanding of the electronic structure of CeF in which the 6p orbital mixes in the 6s spinor, resulting in an extension of the corresponding spinor to the other side from F^-. The same feature is observed in our SA-RASSCF wavefunctions where the 6p orbital mixes in the singly-occupied 6s orbital (6s-6p hybridization), leading to the

extension of the hybridized orbital to the backside of Ce^+ due to the Coulomb repulsion. It is noted that 5d can also hybridize with p-type orbitals to represent a polarization, but the hybridization of 5d was small due to the energy difference between 5d and 6p. Thus, the electronic states of the $[Xe]4f^15d^16s^1$ configuration are relatively stabilized compared to those of the $[Xe]4f^15d^2$ configuration.

Next, we compare the energy levels of the quartet states from the $[Xe]4f^15d^16s^1$ and $[Xe]4f^15d^2$ configurations calculated for CeF without SOCI and with SOCI shown in Fig. 5. The SOCI has brought a mixing of the spin-orbit uncoupled states of CeF, leading to more complexity of the electronic states. The number of the electronic states showing the mixing of $[Xe]4f^15d^16s^1$ and $[Xe]4f^15d^2$ configurations (indicated by green lines) increases to 20. There are 420 (= 105 × 4) independent electronic states originating from quartet states for CeF in a range of 0–4 eV where 56 electronic states in the lowest-lying region (0–0.62 eV) derived by the SOCI calculations correspond to those of the $[Xe]4f^15d_{\pm2}^16s^1$ configuration.

Hence, we focus on this lowest-lying energy region of CeF, and carried out SA-RASSCF/NEVPT2+SOCI calculations for the 56 states (originating from quartet states). In addition, we carried out SA-CASSCF/NEVPT2+SOCI calculations for the 56 states originating from quartet states and the 46 states originating from doublet states, to examine the mixing of quartet and doublet states *via* spin-orbit coupling effects. The number of the doublet states included was determined through a preliminary calculation where the lowest 46 states are lying in a range of 0–0.62 eV at the SA-CASSCF/NEVPT2 level. **Figure 6** shows the energy levels calculated by SA-RASSCF/NEVPT2+SOCI for only quartet states and by SA-CASSCF/NEVPT2+SOCI for both quartet and doublet states, as well as the available

experimental data[10] and previously calculated results by the four-component relativistic scheme with the MCQDPT method.[13] In Fig. 6, the respective electronic states of CeF are distinguished by Ω (quantum number for the total electronic angular momentum around the molecular axis). Experimentally, the ground state of CeF was assigned as Ω = 3.5, and the excitation energies for the electronic states of Ω = 4.5 and 3.5 were reported to be 0.087 and 0.186 eV, respectively. The corresponding values in our SA-RASSCF/NEVPT2+SOCI calculations for only quartet are 0.116 eV (Ω = 4.5) and 0.211 eV (Ω = 3.5), which are in good agreement with the experimental data. By including the mixing with the doublet states in the SOCI calculations, these values are reduced to 0.104 eV (Ω = 4.5) and 0.155 eV (Ω = 3.5), and thus, the former value is in better agreement with the experiment, while the latter show a similar deviation (0.03 eV) from the experiment. The previous four-component relativistic MCQDPT calculations based on the CASCI wavefunction estimated the corresponding energies to be 0.104 eV (Ω = 4.5) and 0.312 eV (Ω = 3.5), and thus, the energy level of the latter state of Ω = 3.5 was overestimated by twice.[13] In their study, only the electronic states of Ω = 1.5, 2.5, 3.5, and 4.5 were calculated to avoid the intruder states, and thus, their result looks sparse compared to our calculations. The present SA-CASSCF/NEVPT2+SOCI calculations show that the ratio of quartet and doublet in the spin-orbit coupled states are 0.986 : 0.014 (the ground state), 0.953 : 0.047 (the excited state with Ω = 4.5), and 0.898 : 0.102 (the excited state with Ω = 3.5), and thus, the mixing from doublet is not so large in these observed states.

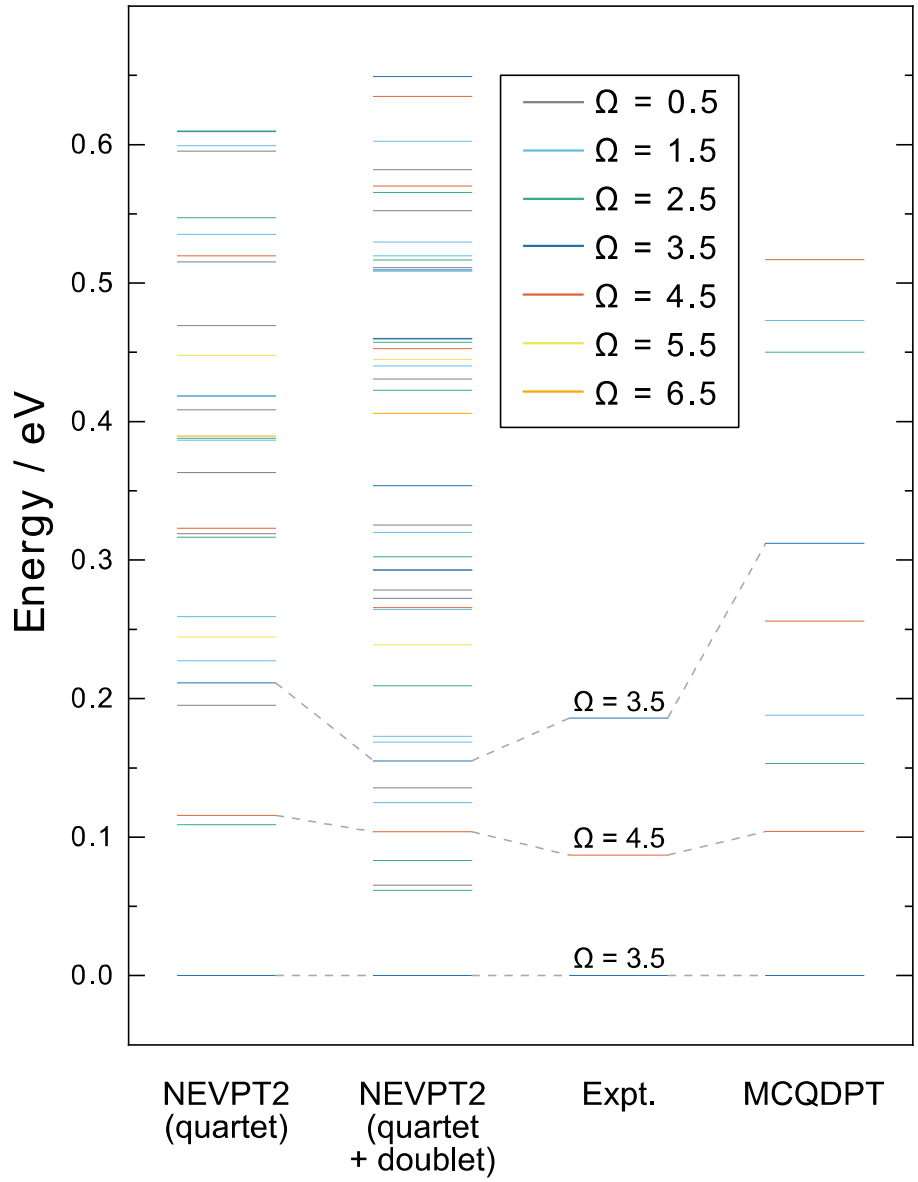

Figure 6. The energy levels of the low-lying electronic states of CeF with the $[Xe]4f^{1}5d^{1}6s^{1}$ configuration at the experimental bond length, r(Ce-F) = 2.048 Å,[36] calculated by SA-RASSCF/NEVPT2+SOCI for quartet and by SA-CASSCF/NEVPT2+SOCI for quartet and doublet. The available experimental data[10] and previous theoretical results by the four-component relativistic method with MCQDPT[13] are also shown.

Finally, the bond length and stretching frequency were calculated for CeF at the SA-RASSCF/NEVPT2+SOCI (for the 56 states from quartet) and SA-CASSCF/NEVPT2+SOCI (for the 56 states from quartet and the 46 states from doublet) levels. In the respective computational levels, the potential energy curves were generated from single-point energy calculations around the equilibrium distance, i.e., in a range of r(Ce-F) = 1.9–2.2 Å with a step of 0.01 Å, and the low-lying rovibrational states were calculated for the ground (Ω = 3.5) and excited (Ω = 4.5) states by numerically solving the rovibrational Schrödinger equation using the MOLCAS program. **Table 2** summarizes the calculated bond lengths and stretching frequencies for CeF with the available experimental data.[10,36] The bond length for the zero-point vibrational state, r_0, is calculated from the corresponding rotational constant, B_0, for $^{140}Ce^{19}F$ in both present calculations and the experiment. In the SA-RASSCF/NEVPT2+SOCI (for quartet) calculations for the ground state, the anharmonicity lengthens the Ce-F bond as r_e = 2.0322 Å to r_0 = 2.0346 Å, and reduces the Ce-F frequency as ν_e = 557.8 cm^{-1} to ν_0 = 554.0 cm^{-1}, and thus, the anharmonicity is not so strong. The calculated bond lengths are shorter by 0.013 Å than the corresponding experimental values, and the calculated stretching frequencies are larger by 10 cm^{-1} than the corresponding experimental values. In the SA-RASSCF/NEVPT2+SOCI (for quartet) calculations for the excited state (Ω = 4.5), the bond length is slightly shorten while the vibrational frequency slightly increases, and this tendency is very consistent with the experimental data. By including the mixing from doublet states, the Ce-F bond length slightly decreases, and the Ce-F stretching frequency slightly increases in both electronic states, and thus, the deviation of the calculated values and the experimental ones becomes slightly larger. It is noted that in the ground state and the target excited state with Ω = 4.5, the mixing weight from doublet states is very small (0.01–0.05) as described

above, and thus, the mixing with double states in SOCI calculations works to make the calculated spectroscopic constants worse, since the weight for the target states in the state-average scheme in SA-CASSCF becomes smaller.

Table 2. The bond length (equilibrium (r_e) and zero-point vibrational state (r_0)), and the vibrational frequency (harmonic one (v_e) and fundamental one (v_0)) of CeF for the ground state ($\Omega = 3.5$) and the excited state ($\Omega = 4.5$), calculated at the SA-RASSCF/NEVPT2+SOCI (for the 56 states from quartet) and SA-CASSCF/NEVPT2+SOCI (for the 56 states from quartet and the 46 states from doublet) levels, with the available experimental data.

	r_e (Å)	r_0 (Å)	v_e (cm^{-1})	v_0 (cm^{-1})
Ground state ($\Omega = 3.5$)				
NEVPT2 (quartet)	2.0322	2.0346	557.8	554.0
NEVPT2 (quartet+doublet)	2.0313	2.0338	560.1	558.1
Expt.[10,36]	–	2.0478	–	543.76
Excited state ($\Omega = 4.5$)				
NEVPT2 (quartet)	2.0311	2.0335	558.1	554.2
NEVPT2 (quartet+doublet)	2.0287	2.0316	558.9	558.6
Expt.[10]	–	2.0471	–	544

Conclusions

In the present study, we performed a systematic calculation of the energy levels of the electronic states of Ce^+ and CeF, which originate from the $4f^15d^16s^1$ and $4f^15d^2$ configurations of Ce^+, to examine the accuracy of *ab initio* computations based on all-electron and effective-core approaches. The significant factors for accurate computations of the electronic structures of the lanthanide-contained molecules are the static and dynamic correlation effects, the scalar and spin-orbit relativistic effects, and the existence of multi-states within a small energy range due to an open-shell character with a high-spin multiplicity occupying 4f, 5d, and 6s orbitals. These complex factors require a state-of-the-art *ab initio* methodology including a good-quality basis set and a multi-configurational/multi-reference wavefunction. One of the authors developed all-electron basis set family, Sapporo-basis-set, which are also tested in this study. In the first part, we carried out SA-RASSCF(SA-CASSCF)/NEVPT2 calculations without and with the spin-orbit coupling effects, for 420 electronic states of Ce^+, originating from $4f^15d^16s^1$ and $4f^15d^2$ quartet configurations. The mixing from doublet states through spin-orbit coupling was also examined, and it is shown that the inclusion of doublet-quartet mixing by spin-orbit coupling is essential to reproduce the energetics of the ground and low-lying excited states. Through comparisons with available experimental data, we decided to employ the SA-RASSCF(SA-CASSCF)/NEVPT2+SOCI method with the Sapporo-QZP basis set, and applied it to the CeF diatomic molecule in the second part. The excitation energies, the equilibrium bond length, and the vibrational frequency are well reproduced by our computations, and we believe that the

present demonstration provides a standard theoretical approach for the lanthanide-contained molecules.

Acknowledgments

This work was supported by JSPS KAKENHI with Grant Number 16KT0047, and partly supported by MEXT as "Priority Issue on Post-K computer" (Development of new fundamental technologies for high-efficiency energy creation, conversion/storage and use). Some of calculations were performed using the Research Center for Computational Science, Okazaki, Japan.

References

[1] M. Dolg (Ed.), Computational Methods in Lanthanide and Actinide Chemistry, John Wiley & Sons, 2015.

[2] M. Bottrill, L. Kwok, and N. J. Long, Chem. Soc. Rev., **35**, 557 (2006).

[3] S. Calvello, M. Piccardo, S. V. Rao, and A. Soncini, J. Comput. Chem., (2017), DOI: 10.1002/jcc.25113.

[4] W. C. Elmler, R. B. Ross, and P. A. Christiansen, Adv. Quant. Chem., **19**, 139 (1988).

[5] E. Sanoyama, H. Kobayashi, and S. Yabushita, J. Mol. Struct. (Theochem), **451**, 189 (1998).

[6] T. Tsuchiya, T. Taketsugu, H. Nakano, and K. Hirao, J. Mol. Struct. (Theochem), **461**, 203 (1999).

[7] I. Gotkis, J. Phys. Chem., **95**, 6086 (1991).

[8] L. A. Kaledin, C. Linton, T. E. Clarke, and R. W. Field, J. Mol. Spectrosc., **154**, 417 (1992).

[9] A. L. Kaledin, M. C. Heaven, R. W. Field, and L. A. Kaledin, J. Mol. Spectrosc., **179**, 310 (1996).

[10] J. C. Bloch, M. C. McCarthy, R. W. Field, and L. A. Kaledin, J. Mol. Spectrosc., **177**, 251 (1996).

[11] W. C. Martin, R. Zalubas, and L. Hagan, Atomic Energy Levels: The Rare-Earth Elements (the Spectra of Lanthanum, Cerium, Praseodymium, Neodymium, Promethium, Samarium, Europium, Gadolinium, Terbium, Dysprosium, Holmium, Ebrium, Thulium, Ytterbium, and Lutetium) (National Bureau of Standards, Washington, D.C., 1978).

[12] Y. Wasada-Tsutsui, Y. Watanabe, and H. Tatewaki, J. Phys. Chem. A, **111**, 8877 (2007).

[13] H. Tatewaki, S. Yamamoto, Y. Watanabe, and H. Nakano, J. Chem. Phys., **128**, 214901 (2008).

[14] T. Nakajima and K. Hirao, Chem. Phys. Lett., **302**, 383 (1999).

[15] B. A. Hess, Phys. Rev. A, **33**, 3742 (1986).

[16] T. Nakajima, K. Hirao, J. Chem. Phys., **113**, 7786 (2000).

[17] M. Sekiya, T. Noro, T. Koga, and T. Shimazaki, Theor. Chem. Acc., **131**, 1247 (2012).

[18] B. O. Roos, R. Lindh, P.-Å. Malmqvist, V. Veryazov, P.-O. Widmark, and A. C. Borin, J. Phys. Chem. A, **112**, 11431 (2008).

[19] Q. Lu and K. A. Peterson, J. Chem. Phys., **145**, 54111 (2016).

[20] T. Noro, M. Sekiya, and T. Koga, Theor. Chem. Acc., **131**, 1124 (2012).

[21] T. Noro, M. Sekiya, and T. Koga, Theor. Chem. Acc., **132**, 1363 (2013).

[22] T. Noro, Segmented GTF basis set factory. http://sapporo.center.ims.ac.jp/sapporo/ (accessed December 8, 2017).

[23] G. Schoendorff and A.K. Wilson, J. Chem. Phys., **140**, 224314 (2014).

[24] M. Dolg, H. Stoll, and H. Preuss, J. Chem. Phys., **90**, 1730 (1989).

[25] R. Gulde, P. Pollak, and F. Weigend, J. Chem. Theo. Comput., **8**, 4062 (2012).

[26] A. Wolf, M. Reiher, and B. A. Hess, J. Chem. Phys., **117**, 9215 (2002).

[27] H.-J. Werner, P. J. Knowles, G. Knizia, F. R. Manby, and M. Schütz, Wiley Interdiscip. Rev. Comput. Mol. Sci., **2**, 242 (2012).

[28] H.-J. Werner, P. J. Knowles, G. Knizia, F. R. Manby, M. Schütz, P. Celani, T. Korona, R. Lindh, A. Mitrushenkov, G. Rauhut, K. R. Shamasundar, T. B. Adler, R. D. Amos, A. Bernhardsson, A. Berning, D. L. Cooper, M. J. O. Deegan, A. J. Dobbyn, F. Eckert, E. Goll, C.

Hampel, A. Hesselmann, G. Hetzer, T. Hrenar, G. Jansen, C. Köppl, Y. Liu, A. W. Lloyd, R. A. Mata, A. J. May, S. J. McNicholas, W. Meyer, M. E. Mura, A. Nicklass, D. P. O'Neill, P. Palmieri, D. Peng, K. Pflüger, R. Pitzer, M. Reiher, T. Shiozaki, H. Stoll, A. J. Stone, R. Tarroni, T. Thorsteinsson, and M. Wang, (2012).

[29] J. Olsen, B. O. Roos, P. Jørgensen, and H. J. A. Jensen, J. Chem. Phys., **89**, 2185 (1988).

[30] C. Angeli, R. Cimiraglia, S. Evangelisti, T. Leininger, and J.-P. Malrieu, J. Chem. Phys., **114**, 10252 (2001).

[31] C. Angeli, R. Cimiraglia, and J. P. Malrieu, J. Chem. Phys., **117**, 9138 (2002).

[32] C. Angeli, M. Pastore, and R. Cimiraglia, Theor. Chem. Acc., **117**, 743 (2007).

[33] A. Berning, M. Schweizer, H.-J. Werner, P. J. Knowles, and P. Palmieri, Mol. Phys., **98**, 1823 (2000).

[34] Y. Ono, Y. Kondo, M. Kobayashi, and T. Taketsugu, Chem. Lett., **45**, 478 (2016).

[35] F. Aquilante, L. De Vico, N. Ferré, G. Ghigo, P.-Å. Malmqvist, P. Neogrády, T. B. Pedersen, M. Pitoňák, M. Reiher, B. O. Roos, L. Serrano-Andrés, M. Urban, V. Veryazov, and R. Lindh, J. Comput. Chem., **31**, 224 (2010).

[36] Y. Azuma, W. J. Childs, and K. L. Menningen, J. Mol. Spectrosc., **145**, 413 (1991).